



## Short communication

Biosensor based on chemically-designed anchorable cytochrome *c* for the detection of H<sub>2</sub>O<sub>2</sub> released by aquatic cellsGuillaume Suárez<sup>a,\*</sup>, Christian Santschi<sup>a</sup>, Olivier J.F. Martin<sup>a</sup>, Vera I. Slaveykova<sup>b</sup><sup>a</sup> Nanophotonics and Metrology Laboratory, Swiss Federal Institute of Technology Lausanne (EPFL), EPFL-STI-NAM, Station 11, CH-1015 Lausanne, Switzerland<sup>b</sup> Institute F.A. Forel, University of Geneva, Route de Suisse 10, PO Box 416, CH-1290 Versoix, Switzerland

## ARTICLE INFO

## Article history:

Received 20 August 2012

Received in revised form

19 October 2012

Accepted 26 October 2012

Available online 10 November 2012

## Keywords:

Cytochrome *c*

Bioelectrochemistry

Direct electron transfer

Chemical manipulation

Oxidative stress

Aquatic cells

## ABSTRACT

A novel third generation biosensor was developed based on one-shot adsorption of chemically-modified cytochrome *c* (cyt *c*) onto bare gold electrodes. In contrast to the classic approach which consists of attaching cyt *c* onto an active self-assembled monolayer (SAM) previously chemisorbed on gold, here short-chain thiol derivatives (mercaptopropionic acid, MPA) were chemically introduced on cyt *c* protein shell via its lysine residues enabling the very fast formation (< 5 min) of an electroactive biological self-assembled monolayer (SAM) exhibiting a quasi-reversible electrochemical behavior and a fast direct electron transfer (ET). The heterogeneous ET rate constant was estimated to be  $k_s = 1600 \text{ s}^{-1}$ , confirming that short anchors facilitate the ET via an efficient orientation of the heme pocket. In comparison, no ET was observed in the case of native and long-anchor (mercaptoundecanoic acid, MUA) modified cyt *c* directly adsorbed on gold. However, in both cases the ET was efficiently restored upon in-bulk generation of gold nanoparticles which acted as electron shuttles. This observation emphasizes that the lack of electroactivity might be caused by either an inappropriate orientation of the protein (native cyt *c*) or a critical distance (MUA-cyt *c*). Finally, the sensitivity of the bare gold electrode directly modified with MPA-cyt *c* to hydrogen peroxide (H<sub>2</sub>O<sub>2</sub>) was evaluated by amperometry and the so-made amperometric biosensor was able to perform real-time and non-invasive detection of endogenous H<sub>2</sub>O<sub>2</sub> released by unicellular aquatic microorganisms, *Chlamydomonas reinhardtii*, upon cadmium exposure.

© 2012 Elsevier B.V. All rights reserved.

## 1. Introduction

Over the last two decades amperometric biosensors based on the enzymatically-catalyzed reduction of H<sub>2</sub>O<sub>2</sub> have attracted a broad interest caused by their accurate sensitivity and specificity. In such an approach, the analytical performance of the biosensor is strongly determined by the electron transfer (ET) efficiency between the electrode material and the immobilized heme-containing protein that exhibits peroxidase (or pseudo-) activity. Therefore, in the case of the so-called third generation biosensors which rely on direct ET the ability to achieve an efficient electrical communication resorts to orientation and distance issues between the electrode surface and the protein redox center (Gorton et al., 1999). Among the large hemoprotein family, cytochrome *c* (cyt *c*) is a globular redox protein with 12.4 kDa molecular weight that is involved in cellular electron transfer pathways. Thanks to its pseudo-peroxidase activity cyt *c* has been used to detect H<sub>2</sub>O<sub>2</sub> in biochemical assays (Vandewalle and

Petersen, 1987) or electrochemical biosensors (Zhao et al., 2005). However, it is also known that cyt *c* exhibits a very low ET once in contact with solid bare electrodes which results in a poor electrochemical behavior presumably caused by protein denaturing (Allen et al., 1997). Thus, a number of studies have focused on the modification of the gold electrode surface in order to generate a suitable molecular environment that prevents cyt *c* from denaturing and enhances the ET rate constant. One approach consists of modifying the gold electrode surface with a chemisorbed self-assembled monolayer (SAM) of alkanethiols that exhibit a carboxylic headgroup at the solution interface (Tanimura et al., 2002). In this case, the strategy relies on the attractive interaction taking place between the negatively charged carboxylates and the region at the vicinity of the heme pocket which contains five positively charged lysine residues (Nakano et al., 2007). The efficient orientation and immobilization of cyt *c* on the electrode via the promoter SAM results in an enhanced ET that is distance-independent for short chains and then decreases exponentially when the SAM length increases, as expected for a tunneling mechanism. The addition of mercaptoalcohol to form compact mixed SAM provides an even more favorable environment to display fast ET rate constants (Davis et al., 2008; Lisdat

\* Corresponding author. Tel.: +41 21 693 68 71; fax: +41 21 693 47 46.  
E-mail address: [guillaume.suarez@epfl.ch](mailto:guillaume.suarez@epfl.ch) (G. Suárez).

and Karube, 2002). Another approach relies on the use of small diameter ( $< 5$  nm) gold nanoparticles (AuNPs) with immobilized on the electrode surface as efficient electron relays that facilitate long-range cyt *c* interfacial ET. In the best cyt *c*-AuNP hybrid system described by Jensen et al. (2007) the ET rate constant is enhanced by one order of magnitude compared to the AuNP-free configuration. A similar effect has also been demonstrated in self-assembled multilayer configurations where cyt *c* undergoes fast ET once immobilized into a hybrid matrix made of AuNP (13 nm diameter) coated with thiolated ssDNA (Zhao et al., 2008). In general, most of the strategies applied to enhance cyt *c* ET rely on engineering the electrode surface with functional SAMs or more complex hybrid/polymeric architectures (Beissenhirtz et al., 2004; Dronov et al., 2008; Jia et al., 2002). However, despite the well standardized approach based on gold modification with functional SAMs prior protein attachment, the modification engineering of proteins by introducing reactive groups such as thiols or other tags, represents an important research area in vivid development (Suárez et al., 2007; Della Pia et al., 2011; McMillan et al., 2002; Holland et al., 2011; So et al., 2009). So far, this protein engineering is mainly based on genetic engineering techniques like site-directed mutagenesis or transpeptidase Y that enable the direct chemisorption of recombinants on bare gold. In that context, the possibility to modify the cyt *c* protein shell with promoters which facilitate its chemisorption and enhance ET rate constant has been scarcely reported. By analogy to the yeast iso-1-cyt *c* (cyt *c*) which contains a cystein in position C102 (Bortolotti et al., 2006; Heering et al., 2004), Andolfi et al. (2007) succeeded in replacing the side chain T102 of cyt *c* with a cystein via site-directed mutagenesis but the resulting mutant remained electroinactive.

Considering this prior art, our strategy reports a chemical alternative that relies on a thiol-modified cyt *c* which spontaneously forms, within 5 min, a chemisorbed electroactive layer that exhibits a very high heterogeneous ET rate constant. The introduction of thiol derivatives—via chemical coupling on cyt *c* lysine residues—that act as anchors on gold prevents protein denaturing and enables controllable “tuning” of the ET rate with the chain length. The so-made amperometric biosensor enabled real-time and non-invasive detection of extracellular  $H_2O_2$  released by unicellular aquatic microorganisms *Chlamydomonas reinhardtii* as a consequence of cadmium-induced oxidative stress.

## 2. Materials and methods

### 2.1. Chemicals

N-(3-dimethylaminopropyl)-N'-ethylcarbodiimide hydrochloride (EDC), N-hydroxysuccinimide (NHS), 3-mercaptopropionic acid (MPA), 11-mercaptopundecanoic acid (MUA), 4-(2-hydroxyethyl)piperazine-1-ethanesulfonic acid (HEPES), phosphate buffered saline (PBS), hydrogen peroxide, gold(III) chloride hydrate, cadmium ion standard solution (Cd(II)) and bovine heart cytochrome *c* (cyt *c*) were all purchased from Sigma-Aldrich (Buchs; Switzerland).

### 2.2. Electrochemical measurements

Cyclic voltammetric and amperometric measurements were performed on a model  $\mu$ Stat 200 Bipotentiostat (DropSens, LLanera, Spain) using a conventional three-electrode electrochemical cell equipped with Ag/AgCl pseudo-reference electrode and a Pt-disk counter electrode. Either PBS or 10 mM HEPES buffer at pH 7.4 were used as supporting electrolyte.

### 2.3. Chemical modification of cyt *c*

The chemical modification of cyt *c* consisted of reacting its lysine residues with carboxyl-terminated thiol derivatives—either mercaptopropionic acid (MPA) or mercaptopundecanoic (MUA)—via carbodiimide/N-hydroxysuccinimide (EDC/NHS) activation. Typically, 0.5 M solutions of MPA or MUA were prepared into phosphate buffer saline (PBS) pH 7.0 and an equimolar amount of EDC and NHS were added under stirring. Then, 50  $\mu$ L of this solution was mixed with 0.5 mL of 500  $\mu$ M cyt *c* in PBS and left to react while stirring at room temperature. After 2 h, the protein was reduced by addition of ascorbic acid and then purified from reagents excess with a separation column (Sephadex G25; GE Healthcare Life Sciences) before recollection into PBS. The final cyt *c* concentrations were estimated by absorption measurements; stock solutions of 200  $\mu$ M were prepared and stored at 4 °C.

### 2.4. Preparation of Au/cyt *c* electrodes

Prior to modification, gold surfaces were treated with hot “Piranha” solution (7:3 mixture of concentrated  $H_2SO_4$  and 30%  $H_2O_2$ ; caution, piranha reacts violently with organic compounds) for 2 h. Freshly cleaned gold planar electrodes (0.1  $cm^{-2}$  active surfaces) were dipped into PBS electrolyte containing 5  $\mu$ M of either native cyt *c*, MPA-cyt *c* or MUA-cyt *c* for an incubation time ranging from 5 to 60 min. Finally, all cyt *c*-modified electrodes were washed in PBS in order to remove any loosely attached protein and kept at 4 °C until use.

### 2.5. Cell culture conditions

The wildtype unicellular freshwater algae *C. Reinhardtii* were provided by the Canadian Phycological Culture Center. Prior to all experiments algal cells contained in Erlenmeyer flasks were grown exponentially in the “TAP” culture medium to their mid-exponential growth phase, harvested by gentle filtration, washed and recollected in 10 mM HEPES at pH 7.4. Cell numbers and surface areas were determined by a Coulter Multisizer III particle counter (Beckman-Coulter, Inc.) for each experimental run.

## 3. Results and discussion

The electrochemical behavior of the different cyt *c* attached onto gold is illustrated with the corresponding cyclic voltammograms (1) in Fig. 1. As expected for native cyt *c* no faradaic peak developed on the capacitive current whereas a pair of well-defined peak, corresponding to the electrochemical oxidation and reduction of heme group, is visible for cyt *c*-MPA. On the other hand, the cyt *c*-MUA chemisorbed onto gold does not show any sign of ET between the redox center and the electrode. In this first stage it is safe to deduce that the introduction of short anchors (three carbons chain) on the cyt *c* shell enables strong attachment to the bare gold surface and dramatically enhances its electrical communication.

However, the lack of electroactivity observed for native cyt *c* and MUA-cyt *c* might be caused by a combination of several critical factors which are: (i) weak attachment on gold leading to a low surface coverage; (ii) protein denaturing due to unfolding interactions on gold; (iii) high protein shielding caused by inappropriate orientation; and (iv) inefficient ET due to excessive distance between the heme group and the electrode surface.

Therefore, an experiment was carried out in order to elucidate which factors determine the electrochemical behavior of the different electrodes configurations. In other words, the main objective here was to connect efficiently all cyt *c* immobilized at

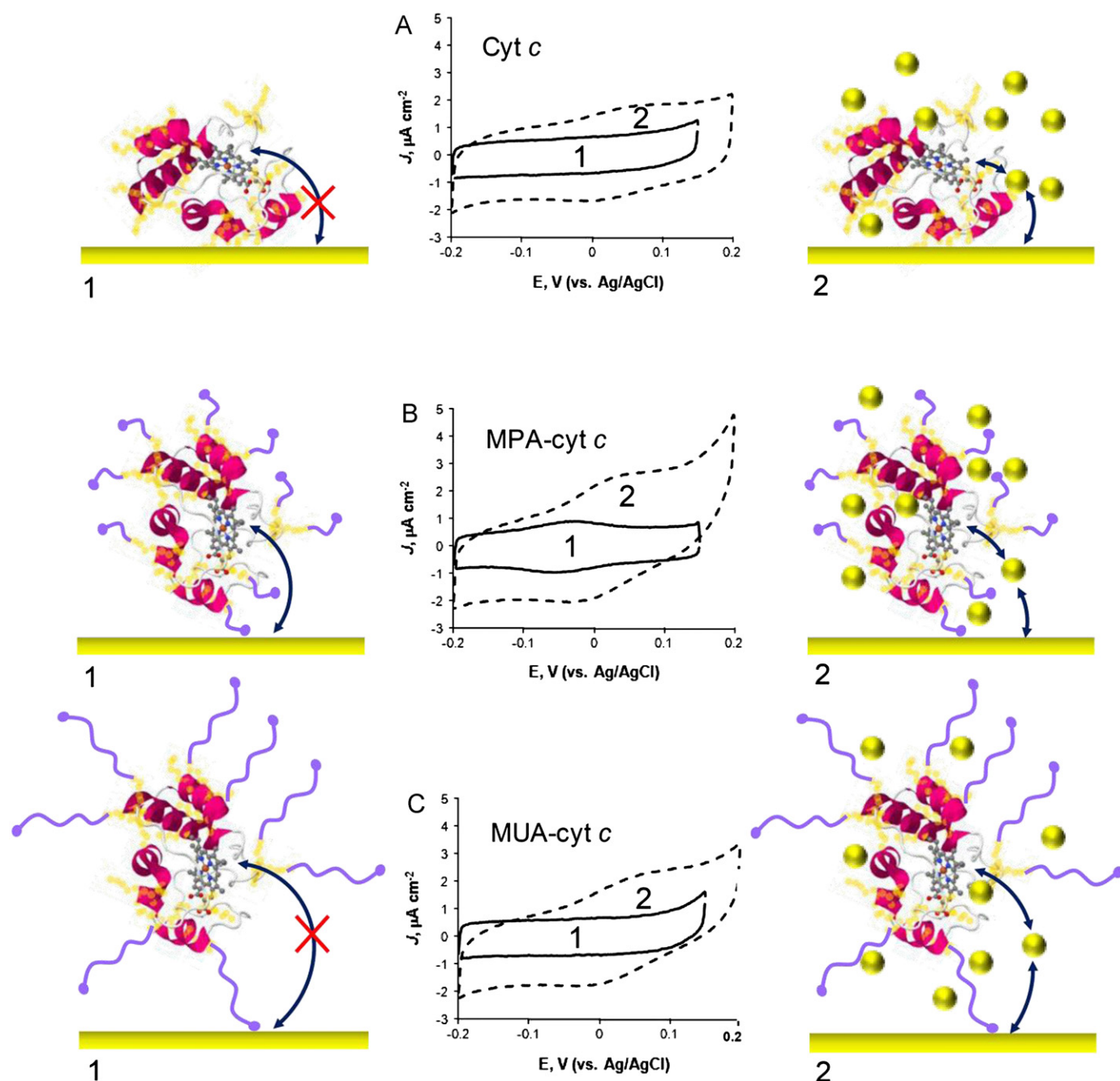


**Fig. 1.** (Center) Cyclic voltammograms obtained for native cyt *c* (A), MPA-cyt *c* (B) and MUA-cyt *c* (C) adsorbed onto bare gold electrodes in the absence (1) or presence (2) of “in-situ” generated gold nanoparticles that act as electron shuttles. (Right and left) Corresponding schematic representation of cyt *c* adsorbed on gold (Lys residues in orange; secondary structure in red and white; MPA or MUA anchors in purple). Black arrows represent the electron transfer between heme group and electrode surface. Experimental conditions: scan rate: 0.05 V s<sup>-1</sup>; supporting electrolyte: PBS; and reference electrode: Ag/AgCl.

the electrode surface independently from their orientation/distance via the addition of electron shuttles in the electrolyte. To that end “in-situ” synthesis of AuNPs was initiated directly in the electrochemical cell upon addition of 100 μM HAuCl<sub>4</sub> and 1 mM 4-(2-hydroxyethyl)piperazine-1-ethanesulfonic acid (HEPES) and the cyclic voltammetry was performed 15 min later. The HEPES-induced reduction of auric salt into AuNPs (Xie et al., 2007) was preferred to the more conventional ascorbic acid method since it has no effect on the redox state of the heme group. The ability of gold nanoparticles to shorten the distance between metalloproteins redox center and the electrode surface has been well reported elsewhere (Abad et al., 2009; Jensen et al., 2007). A critical parameter to achieve an efficient AuNP-assisted electron

transfer (ET) is the dimension of the nanoparticle that should be able to access the heme pocket with no major steric hindrance. Therefore, the “in-situ” generation of AuNPs represents a more opportunistic configuration where particles are formed from seeds to clusters, which then grow up into bigger nanoparticles. In that case, we ensured to generate particles with the appropriate size to make their way to the heme pocket and contribute to connect it to the gold surface. As expected, the presence of AuNPs acting as electron relays between cyt *c* and the electrode strongly modified the cyclic voltammograms previously reported.

As shown in Fig. 1(2), the presence of AuNPs induces a broadening of the capacitive current that reveals an increase of the electrode effective dimensions. Furthermore, for each

electrode configuration, a quasi-reversible pair of peaks is now clearly visible which evidences the presence of active cyt *c* at the gold surface. Those results bring unexpected information on the state of the different cyt *c* adsorbed on the electrode. Contrary to the common belief the lack of electroactive behavior of native cyt *c* cannot be exclusively attributed to the irreversible denaturing effect of physisorption on bare gold, since ET is recovered when free-diffusing AuNPs shuttle the electrons through the system. It is more likely that the direct physisorption favours an inappropriate orientation of the protein where the amino acid shell acts as a shielding structure that prohibits ET. An alternative explanation has to be found in the case of MUA-cyt *c* where the distance between the redox center and the electrode surface is increased with longer anchors. Here the heme-surface distance is certainly the limiting factor for an interfacial ET mechanism to take place. However, diffusing AuNPs shortcut the critical distance and the ET rate constant becomes a combination of interfacial ET mechanisms between cyt *c* and AuNP and a diffusion-limited ET enabled by the AuNP/electrode system (Abad et al., 2009; Jensen et al., 2007). In the case of MPA-cyt *c* chemisorbed on gold the more noticeable change observed in the voltammetric response after generation of AuNPs is an increase of the peak separation indicative of a slower ET rate constant. This result confirms that fast interfacial ET mechanisms are predominant for electroactive MPA-cyt *c* as a result of a favorable orientation on gold. Once AuNPs are present in the system the badly oriented MPA-cyt *c* also contributes to the electrical response, which then enters a diffusion-limited ET regime.

The voltammetric monitoring of MPA-cyt *c* chemisorption on bare gold emphasizes the rapidity of the electroactive protein layer formation with the maximum peak intensity reached within 5 min (20 cycles at  $\nu=0.05 \text{ V s}^{-1}$ ), as shown in Fig. 2A. Moreover, the analysis of the peaks intensity shows a reversible electrochemical behavior with a value of  $I_a/I_c=0.96$ . The calculation of the  $E_{\text{FWHM}}=86 \text{ mV}$  which is below the theoretical value of  $90.6 \text{ mV}$  defines a Nernstian mono-electronic process strongly

adsorbed on the electrode surface (Laviron, 1982). The surface coverage of electroactive MPA-cyt *c* on gold was estimated to be  $\Gamma=4 \times 10^{-12} \text{ mol cm}^{-2}$  which corresponds roughly to 25% of the theoretical value reported by Nakano et al. (2007) for a fully packed cyt *c* surface coverage. It is also observable that the formal potential  $E^0=-48 \text{ mV}$  (vs. Ag/AgCl) is negative-shifted as compared to native cyt *c* in solution, as expected for a covalently immobilized protein (Yue and Waldeck, 2005). Furthermore, cyclic voltammetry was performed at different scan rates in order to study the ET mechanism taking place at a MPA-cyt *c* modified electrode. The voltammograms in Fig. 2B show the influence of the scan rate both on the peak current intensity and the peak-to-peak separation. As depicted in Fig. 2C the anodic and cathodic peak currents are linearly proportional to the scan rate in the range between  $0.01$  and  $0.6 \text{ V s}^{-1}$ , which is expected for a surface-controlled electrochemical process. An estimated value of the heterogeneous ET rate constant,  $k_s$ , has been calculated from the analysis of peak-to-peak separations using Laviron's method (Laviron, 1979). Considering a charge transfer coefficient  $\alpha=0.5$  a high value of  $k_s=1600 \text{ s}^{-1}$  was calculated, which is in good agreement with those reported for cyt *c* covalently attached onto a SAM of mercaptobutyric acid (de Groot et al., 2007) or a mixed SAM of MPA/mercaptoethanol (Davis et al., 2008).

The characterization of MPA-cyt *c* modified electrode was further extended in order to evaluate its analytical performances for  $\text{H}_2\text{O}_2$  detection. The electrocatalytic current generated at the poised electrode surface ( $E_{\text{app}}=-0.15 \text{ V}$  vs. Ag/AgCl) upon addition of increasing  $\text{H}_2\text{O}_2$  concentration was measured via standard amperometric technique. The corresponding calibration curve (Supplementary information, Fig. S1) exhibits a linear dynamic range from  $0$  to  $250 \mu\text{M}$  of  $\text{H}_2\text{O}_2$  with a limit-of-detection evaluated at  $1 \mu\text{M}$  ( $S/N=3$ ). Finally, the apparent Michaelis-Menten constant was determined using Hanes-Woolf plot and found to be  $K_{\text{app}}=33 \mu\text{M}$ . This low value for  $K_{\text{app}}$  reflects the high  $\text{H}_2\text{O}_2$  affinity exhibited by the immobilized MPA-cyt *c*.

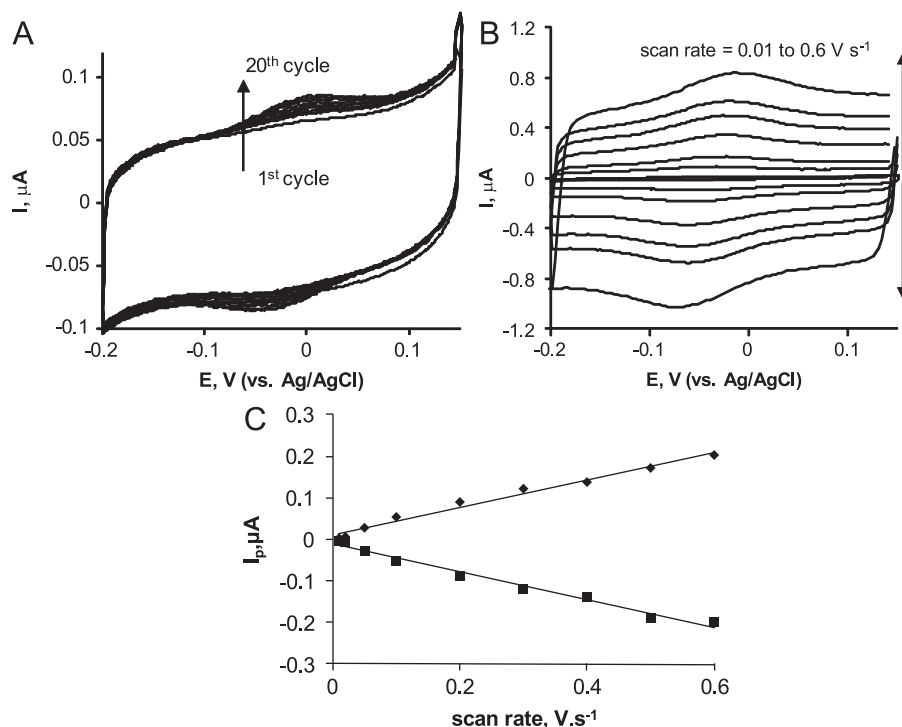


**Fig. 2.** (A) Cyclic voltammograms obtained with gold electrodes in contact with MPA-cyt *c* solution ( $5 \mu\text{M}$ ) for 20 cycles at  $\nu=0.05 \text{ V s}^{-1}$ ; (B) cyclic voltammograms of MPA-cyt *c*/Au electrode at different scan rates ranging from  $\nu=0.01$  to  $0.6 \text{ V s}^{-1}$ ; (C) Typical peak intensity dependence on the scan rate plot, from the experimental data in panel of (B). Experimental conditions: supporting electrolyte: PBS and reference electrode: Ag/AgCl.

McNeil et al. have demonstrated in several works that cytochrome *c*-based amperometric biosensors can efficiently perform real-time detection of free radical superoxide produced by stimulated cell lines (Henderson et al., 2009; Manning et al., 1998). However, despite being fast, specific, and sensitive, this technique remained largely under-use in the field of ecotoxicology. Here, the developed biosensor was further applied for real-time detection of  $\text{H}_2\text{O}_2$  overproduction in aquatic microorganisms upon cadmium addition. *C. reinhardtii* was chosen as a model green microalga representative of the freshwater phytoplankton. The effect of Cd(II) on *C. reinhardtii* has already been studied with techniques involving standard ROS-specific probes (Szivak et al., 2009) or proteomic/genomic analysis (Hutchins et al., 2010; Simon et al., 2008). The presence of sub-lethal concentrations of Cd(II) induces an overproduction of ROS and, as a consequence, the level of antioxidants becomes up-regulated (Hanikenne, 2003; Simon et al., 2008). In the case of phytoplanktonic cells such as *C. reinhardtii*, the protective role played by the additional cell-wall prevents the most reactive ROS that are the oxygen and nitrogen radicals to reach the extracellular environment. Consequently, only  $\text{H}_2\text{O}_2$  excess is able to diffuse through the cell-wall

into the extracellular environment. To explore the capabilities of this novel biosensor to detect the changes of  $\text{H}_2\text{O}_2$  concentrations in the extracellular environment, bare gold electrodes were modified with MPA-cyt *c* via a fast incubation step (15 min) and then rinsed. Suspension containing  $10^6$  cells  $\text{mL}^{-1}$  *C. reinhardtii* in the mid-exponential growth phase in 10 mM HEPES at pH 7.4 were prepared. Aliquots of 30  $\mu\text{L}$  of algal suspensions were placed into the sensing chamber. The amperometric measurements were performed at  $E_{\text{app}} = -0.15$  V (vs. Ag/AgCl) and at room temperature. In Fig. 3B, the current response profile in absence of Cd(II) is stable and caused by the capacitive current. Addition of 1  $\mu\text{M}$  of Cd(II) results in a rapid and a progressive increase of the cathodic current which provides evidence for the presence of  $\text{H}_2\text{O}_2$  that oxidizes MPA-cyt *c* at the electrode surface. This result clearly demonstrates that the developed biosensor is a well suited tool for non-invasive and real-time detection of endogenous  $\text{H}_2\text{O}_2$  in the extracellular medium; it can be used to measure the oxidative status of phytoplankton cells non-invasively.

#### 4. Conclusion

The chemical introduction of thiol derivatives in the cytochrome *c* structure enables its fast chemisorption (< 5 min) onto bare gold electrodes. Most importantly, the self-adsorbed cytochrome *c* shows a quasi-reversible electrochemical behavior with an estimated heterogeneous ET rate constant particularly high ( $k_s = 1600$   $\text{s}^{-1}$ ). This novel third generation biosensor displays reliable analytical performances for  $\text{H}_2\text{O}_2$  detection and exhibits a linear response up to 250  $\mu\text{M}$ . Using the developed biosensor it has been possible to detect in real-time and non-invasively the  $\text{H}_2\text{O}_2$  overproduced by phytoplanktonic cells in response to Cd(II) exposure. Furthermore, the one-shot biofunctionalization procedure demonstrated here might also be useful for a broad variety of gold transducers, as well as for many biosensing applications.

#### Acknowledgment

This work was supported by the Swiss National Science Foundation (Projects CR2312\_130164 and 406440\_131280 in the framework of the Swiss National Research Program NRP 64).

#### Appendix A. Supporting information

Supplementary data associated with this article can be found in the online version at <http://dx.doi.org/10.1016/j.bios.2012.10.083>.

#### References

- Abad, J.M., Gass, M., Bleloch, A., Schiffrin, D.J., 2009. *Journal of the American Chemical Society* 131, 10229–10236.
- Allen, H., Hill, O., Hunt, N.I., Bond, A.M., 1997. *Journal of Electroanalytical Chemistry* 436, 17–25.
- Andolfi, L., Caroppi, P., Bizzarri, A.R., Piro, M.C., Sinibaldi, F., Ferri, T., Polticelli, F., Cannistraro, S., Santucci, R., 2007. *Protein Journal* 26, 271–279.
- Beissenhirtz, M.K., Scheller, F.W., Lisdat, F., 2004. *Analytical Chemistry* 76, 4665–4671.
- Bortolotti, C.A., Battistuzzi, G., Borsari, M., Facci, P., Ranieri, A., Sola, M., 2006. *Journal of the American Chemical Society* 128, 5444–5451.
- Davis, K.L., Drews, B.J., Yue, H., Waldeck, D.H., Knorr, K., Clark, R.A., 2008. *Journal of Physical Chemistry C* 112, 6571–6576.
- de Groot, M.T., Evers, T.H., Merkk, M., Koper, M.T.M., 2007. *Langmuir* 23, 729–736.
- Della Pia, E.A., Elliott, M., Jones, D.D., MacDonald, J.E., 2011. *ACS Nano* 6, 355–361.
- Dronov, R., Kurth, D.G., Mohwald, H., Scheller, F.W., Friedmann, J., Pum, D., Sleytr, U.B., Lisdat, F., 2008. *Langmuir* 24, 8779–8784.

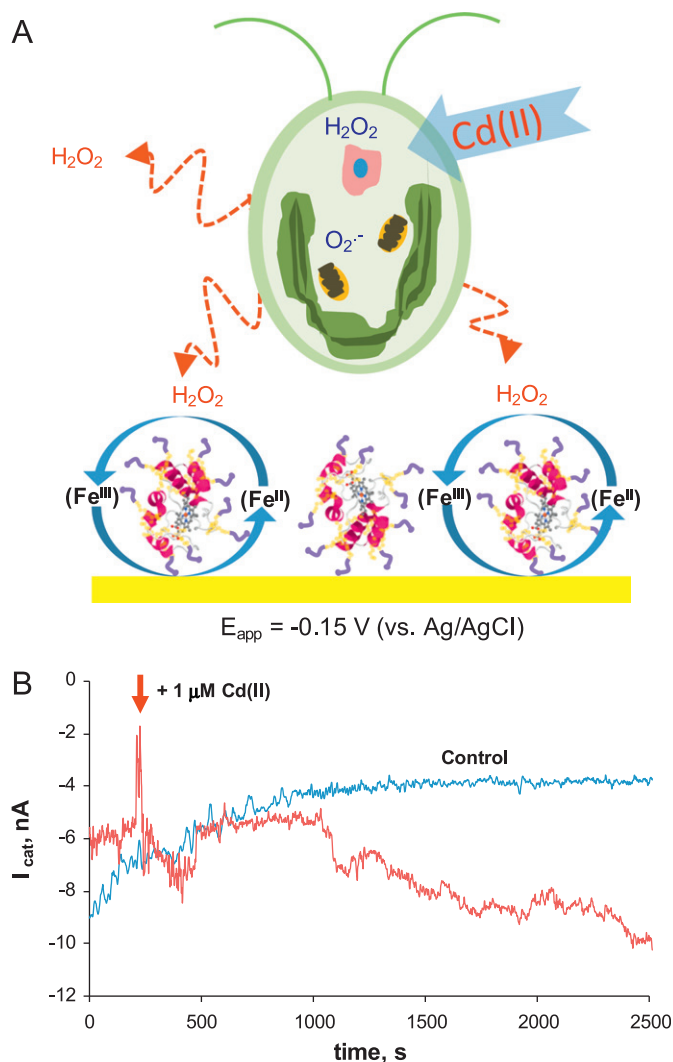


**Fig. 3.** (A) Schematic representation of extracellular detection of  $\text{H}_2\text{O}_2$  released by *C. reinhardtii* upon Cd(II)-induced oxidative stress using the MPA-cyt *c*/Au biosensor. (B) Amperometric real-time detection of  $\text{H}_2\text{O}_2$  as a response to Cd(II) addition into the sensing chamber (indicated by the arrow). Experimental conditions:  $E_{\text{app}} = -0.15$  V (vs. Ag/AgCl) and *C. reinhardtii*:  $10^6$  cells  $\text{mL}^{-1}$  in HEPES 10 mM pH 7.4.

- Gorton, L., Lindgren, A., Larsson, T., Munteanu, F.D., Ruzgas, T., Gazaryan, I., 1999. *Analytica Chimica Acta* 400, 91–108.
- Hanikenne, M., 2003. *New Phytologist* 159, 331–340.
- Heering, H.A., Wiertz, F.G.M., Dekker, C., de Vries, S., 2004. *Journal of the American Chemical Society* 126, 11103–11112.
- Henderson, J.R., Swalwell, H., Boulton, S., Manning, P., McNeil, C.J., Birch-Machin, M.A., 2009. *Free Radical Research* 43, 796–802.
- Holland, J.T., Lan, C., Brozic, S., Atanassov, P., Banta, S., 2011. *Journal of the American Chemical Society* 133, 19262–19265.
- Hutchins, C.M., Simon, D.F., Zerges, W., Wilkinson, K.J., 2010. *Aquatic Toxicology* 100, 120–127.
- Jensen, P.S., Chi, Q., Grumsen, F.B., Abad, J.M., Horsewell, A., Schiffrin, D.J., Ulstrup, J., 2007. *Journal of Physical Chemistry C* 111, 6124–6132.
- Jia, J.B., Wang, B.Q., Wu, A.G., Cheng, G.J., Li, Z., Dong, S.J., 2002. *Analytical Chemistry* 74, 2217–2223.
- Laviron, E., 1979. *Journal of Electroanalytical Chemistry* 101, 19–28.
- Laviron, E., 1982. *Electroanalytical Chemistry* 12, 53–157.
- Lisdas, F., Karube, I., 2002. *Biosensors & Bioelectronics* 17, 1051–1057.
- McMillan, R.A., Paavola, C.D., Howard, J., Chan, S.L., Zaluzec, N.J., Trent, J.D., 2002. *Nature Materials* 1, 247–252.
- Manning, P., McNeil, C.J., Cooper, J.M., Hillhouse, E.W., 1998. *Free Radical Biology and Medicine* 24, 1304–1309.
- Nakano, K., Yoshitake, T., Yamashita, Y., Bowden, E.F., 2007. *Langmuir* 23, 6270–6275.
- Simon, D.F., Descombes, P., Zerges, W., Wilkinson, K.J., 2008. *Environmental Toxicology and Chemistry* 27, 1668–1675.
- So, C.R., Tamerler, C., Sarikaya, M., 2009. *Angewandte Chemie International Edition* 48, 5174–5177.
- Suárez, G., Jackson, R.J., Spoons, J.A., McNeil, C.J., 2007. *Analytical Chemistry* 79, 1961–1969.
- Szivak, I., Behra, R., Sigg, L., 2009. *Journal of Phycology* 45, 427–435.
- Tanimura, R., Hill, M.G., Margoliash, E., Niki, K., Ohno, H., Gray, H.B., 2002. *Electrochemical and Solid State Letters* 5, E67–E70.
- Vandewalle, P.L., Petersen, N.O., 1987. *FEBS Letters* 210, 195–198.
- Xie, J.P., Lee, J.Y., Wang, D.I.C., 2007. *Chemistry of Materials* 19, 2823–2830.
- Yue, H.J., Waldeck, D.H., 2005. *Current Opinion in Solid State & Materials Science* 9, 28–36.
- Zhao, G.C., Yin, Z.Z., Zhang, L., Wei, X.W., 2005. *Electrochemistry Communications* 7, 256–260.
- Zhao, J., Zhu, X.L., Lib, T., Li, G.X., 2008. *Analyst* 133, 1242–1245.